Traveling shock front in quasi-two-dimensional granular flows

Guoqi Hu,[1,2] Yinchang Li,[1] Meiying Hou,[1] and Kiwing To[3]
[1]*Beijing National Laboratory for Condensed Matter Physics, Institute of Physics, Chinese Academy of Sciences, Beijing 100190*
[2]*College of Science, Ningbo University of Technology, Ningbo 315016*
[3]*Institute of Physics, Academia Sinica, Taipei 115*
(Received 2 October 2009; published 29 January 2010)

While the density profile of a granular shock front can be obtained by the conventional treatment of supersonic fluids, its temperature profile is very different from that in ordinary shocks. We study the density and temperature profiles of a traveling granular shock generated by piling up metal spheres in a closed bottom quasi-two-dimensional channel. We successfully account for the temperature profile in the granular shock using a simple kinetic theory in terms of energy transfer from the mean flow direction to the transverse direction. Contrary to ordinary fluids and previous granular shock experiments, the granular shock width is found to increase with the inflow rate.

DOI: 10.1103/PhysRevE.81.011305 PACS number(s): 45.70.Qj, 45.70.Mg, 45.70.Vn

Granular flows are common in nature and in industrial processes. Better understanding of granular flow may lead to less damage in natural disasters (such as avalanches and landslides) and huge savings in the transportation of granular materials in chemical and pharmaceutical industries. In granular flows, the particles collide with each other inelastically. This is intrinsically different from ordinary fluids in which the intermolecular interactions are elastic. Nevertheless, in rapid granular flows when the energy dissipated by inelastic collisions is small compared to the mean kinetic energy of the particles, a granular fluid should behave similarly to an ordinary fluid. On the other hand, the mean flow velocity in a rapid granular flow may easily exceed the sound speed of granular fluids [1]. Hence shock fronts with density profiles similar to those in supersonic flow of ordinary gases, are easily generated. In the experiments of Rericha *et al.* [2] and those of Boudet *et al.* [3] the density profiles of the shock front around a stationary obstacle were indeed found to be consistent with those obtained by conventional treatment of supersonic fluids [4]. However, the temperature profiles in the granular shock measured in these experiments are very different from those in ordinary shocks.

While the temperature profile in an ordinary shock is a monotonic increasing function across the shock, the temperature profile of granular shock goes through a peak [3] and the downstream temperature is less than the upstream temperature. To obtain a basic understanding of the granular shock temperature profile, it is better to avoid complications due to three-dimensional flow and the presence of open boundaries. Hence we choose to study the granular shocks generated by the piling up of gravity-driven metal spheres falling in a two-dimensional channel with a closed bottom. The granular shock in such a setup is the result of a dilute-to-dense transition commonly observed in granular flows [5,6], more generally seen in highway traffic [7], pedestrian stream [8], and floating ice [9]. In our setup, a layer of thermally isotropic granular fluid is found between upstream dilute granular gas and granular solids at the bottom of the channel. The nontrivial granular temperature profile is due to the transfer of mean flow energy to thermal energy in this isotropic granular fluid layer. By suitably identifying each particle as belonging either to a dilute granular gas or the isotropic granular fluid, the measured temperature profile is found to be consistent with that calculated using a simple kinetic theory. In addition, contrary to the results from Boudet *et al.* [3], the width of the density profile is found to increase with particle inflow rate.

Our setup consists of two parallel 80-mm-wide and 1.6-m-long glass plates inclined at an angle of 10° from the horizontal plane as shown in Fig. 1. The glass plates are spaced 2.2 mm apart, slightly larger than the diameter of the particles used in our experiments, so that the particles flow in quasi-two-dimensional motion within this inclined channel. A reservoir of particles (steel spheres of diameter of 2.0 mm) is placed at the top of the channel and the rate of particles flowing into the channel is controlled by the size of the opening of the reservoir gate. In our study, six different particle inflow rates (γ=650, 814, 1054, 1367, 1510, and 1890 particles/s) are used. As the particles fill the channel, the boundary of dense region moves up from the bottom in the form of a granular shock. A fast charge-coupled device camera capable of taking 955 images of 256×256 pixel^2 in 1 s is placed to record the images when the granular shock passes the observation section between 4 and 12 cm from the channel bottom. Before the granular shock reaches the top of the observation section, the mean velocity of particles in the dilute granular gas region is 1.24 m/s and the mean density is 1.2×10^{-4} mm^{-2}. This corresponds to a Mach number of 6 for the upstream dilute granular gas [10]. A typical image obtained in the experiment is shown in Fig. 1. Here the flow direction is set as the y direction and the transverse direction as the x direction. From the recorded image sequence, the

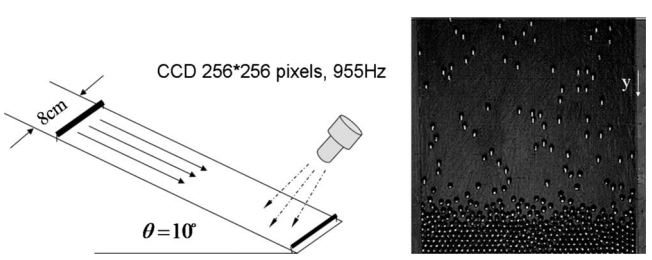

FIG. 1. Schematic diagram of the experimental setup. The photo at the right is a typical image.

 ©2010 The American Physical Society

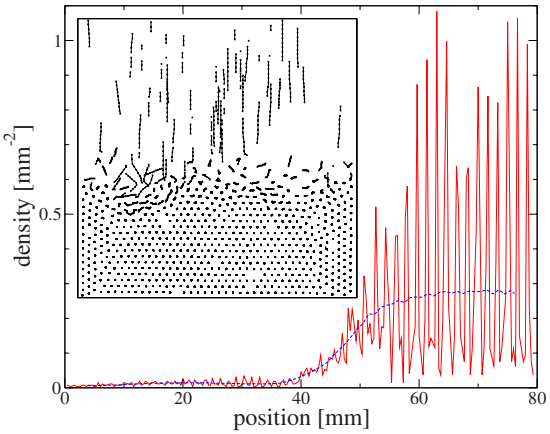

FIG. 2. (Color online) Mean density profile measured during the interval 0.518 s$<t<$0.528 s at inflow rate γ=1367 s^{-1}. The dash line is the running average of the mean profile. The inset shows the trajectories of the particle during this time interval.

trajectory of each particle is extracted and its velocity components (v_x, v_y) are obtained by particle tracking software.

The inset of Fig. 2 shows the trajectories of particles during a time interval 0.518 s$<t<$0.528 s in an experiment of particle inflow rate γ=1367 s^{-1}. One can see three different regions: a dilute granular gas with high mean flow speed at the top, a high density motionless granular solid at the bottom, and a layer of granular fluid between the gas and solid. In the dilute gas region, the velocity variance of the particles in the y direction is found to be larger than that in the x direction. Hence the dilute gas is thermally anisotropic. On the other hand, the granular fluid layer is found to be thermally isotropic: the velocity variances of the particles in both directions are the same. The conversion from the anisotropic dilute gas to the isotropic granular fluid is due to interparticle collisions. Since interparticle collisions are inelastic, all the kinetic energy of the particles in the granular fluid is lost eventually and the granular fluid becomes a granular solid. The crystalline structure of the granular solid is clearly shown by the particle density profile that oscillates rigorously with a mean peak spacing of 1.71 mm (see Fig. 2). When the peaks are filtered out using a running average procedure with a 7 mm window, the mean density of the solid region is found to be n_s=0.276 mm^{-2}. The mean peak spacing and mean density obtained are consistent with those calculated for a triangular close pack arrangement of monodisperse spheres with 2 mm diameter in two dimensions.

Using the running average procedure, we obtain the mean density profiles at different times. These profiles indicate a density shock front moving upwards as shown in Fig. 3. Fitting these profiles to the generic shock wave profile [4],

$$n(y) = \frac{Ae^{(y-y_o)/\lambda} + B}{e^{(y-y_o)/\lambda} + 1}, \tag{1}$$

for molecular fluids [4], we obtain the locations of the shock front (y_o) at different times (see inset of Fig. 3) and derive a shock wave speed of 59.3$\pm$0.8 mm/s. On the other hand, the shock speed u is related to the particle inflow rate γ, the width of the channel w, and the density n_s at the bottom of

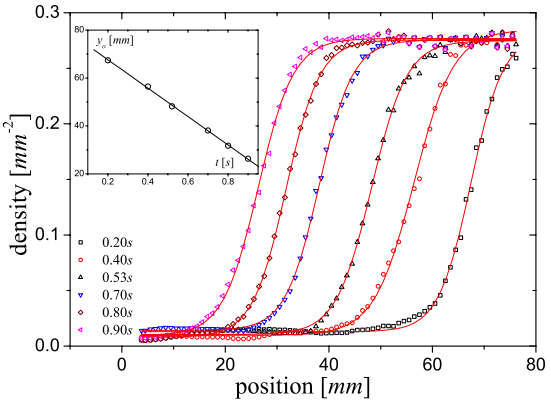

FIG. 3. (Color online) Mean density profiles in the laboratory frame, from right to left: t=0.2, 0.4, 0.52, 0.7, 0.8, and 0.9 s. The inset shows the corresponding positions y_o of the shock front.

the channel by conservation of the mass $u=\frac{\gamma}{n_s w}$. Using the above expression, we have u=58.1$\pm$0.6 mm/s which equals that obtained from the shock front movement within experimental uncertainty. This implies that the density profile is independent of time in the inertial frame moving with speed u. In this comoving frame, the vertical position (y') of the particle at time t will be translated to $y=y'-ut$ and its vertical speed increased by u. We, hereafter, shall present our data in this comoving frame. Note that in the comoving frame, the running average procedure is not needed because the spatial translation procedure has effectively removed the vigorous spatial oscillations found in Fig. 2. Figure 4 shows the density profiles measured at different γ. The inset of this figure shows that the shock width increases with γ. We shall return to this point later.

Figure 5(a) shows the density profile $n(y)$ with an upstream density $A=1.21\times10^{-4}$ mm^{-2} and downstream density of B=0.278 mm^{-2}. The profile reaches the two-dimensional random close pack density [11] n_c=0.267 mm^{-2} at $y=y_s$=40 mm. Hence one expects to find a granular solid in the region $y>y_s$. Figure 5(b) shows

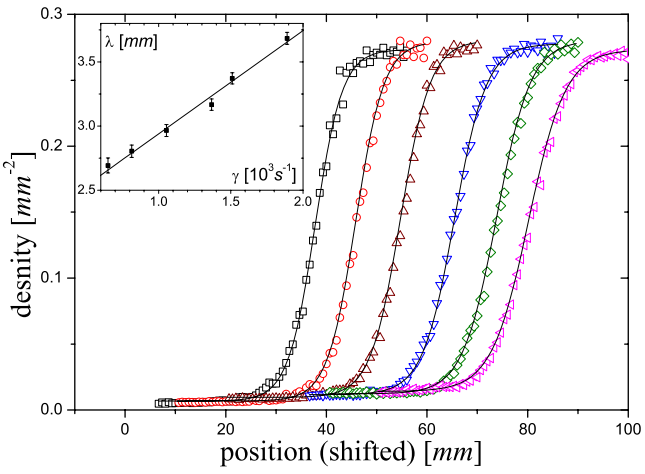

FIG. 4. (Color online) Density profiles at different inflow rates from left to right: γ=650, 814, 1054, 1367, 1510, and 1890 s^{-1}. The inset shows the variation of density profile width λ with γ.

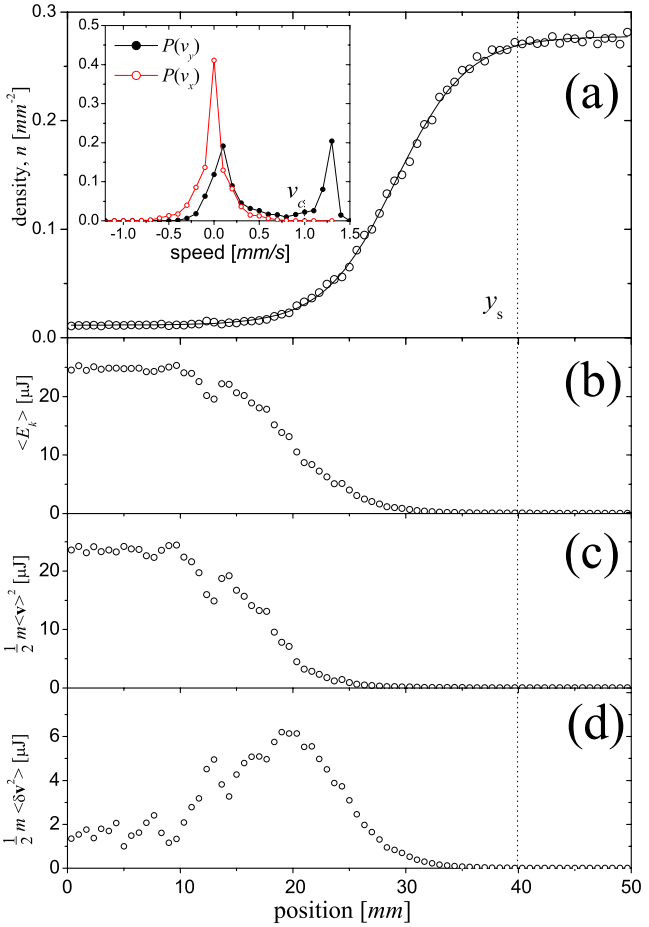

FIG. 5. (Color online) (a) Density n, (b) mean kinetic energy $\langle E_k\rangle$, (c) mean flow $\frac{m}{2}\langle \mathbf{v}\rangle^2$, and (d) thermal kinetic energy profile $\frac{m}{2}\langle \delta\mathbf{v}^2\rangle$ in the comoving frame. The inset in (a) shows the probability functions $P(v_y)$ and $P(v_x)$ at an upstream location.

the measured average kinetic energy per particle $\langle E_k\rangle = \frac{m}{2}\langle \mathbf{v}^2\rangle$ which decreases monotonically from 25 μJ at $y=0$ mm to 0.062 μJ downstream. Since $\langle E_k\rangle$ is the sum of mean flow energy and thermal energy,

$$\langle E_k\rangle = \frac{m}{2}\langle(\langle \mathbf{v}\rangle + \delta\mathbf{v})^2\rangle = \frac{m}{2}(\langle \mathbf{v}\rangle^2 + \langle \delta\mathbf{v}^2\rangle), \tag{2}$$

where $\frac{m}{2}\langle \mathbf{v}\rangle^2$ and $\frac{m}{2}\langle \delta\mathbf{v}^2\rangle$ are, respectively, the mean flow kinetic energy and the thermal kinetic energy of the particles. In the region $y<10$ mm, $\langle E_k\rangle$ is nearly constant. Energy dissipations in this region can be neglected because the rate of interparticle collision is small. In the region 10 mm$<y<$20 mm, $\frac{m}{2}\langle \mathbf{v}\rangle^2$ decreases while $\frac{m}{2}\langle \delta\mathbf{v}^2\rangle$ increases. This suggests a transfer of mean flow energy to thermal energy. Since such energy transfer is mediated by dissipative interparticle collisions, $\langle E_k\rangle$ also decreases in this region. When $y>20$ mm, density is so high that even the thermal energy $\frac{m}{2}\langle \delta\mathbf{v}^2\rangle$ decreases due to increasing collision rate.

In order to gain some quantitative understanding of this energy transfer process, we further decompose $\langle E_k\rangle$ into components in the transverse and mean flow directions so that $\langle E_k\rangle = \frac{m}{2}\langle v_x^2 + v_y^2\rangle = \frac{m}{2}\langle \delta v_x^2 + \langle v_x\rangle^2 + \delta v_y^2 + \langle v_y\rangle^2\rangle$, where $\langle \delta v_x^2\rangle = \langle (v_x - \langle v_x\rangle)^2\rangle$ and $\langle \delta v_y^2\rangle = \langle (v_y - \langle v_y\rangle)^2\rangle$ are the velocity variances in the transverse and mean flow directions, respectively. Since $\langle v_x\rangle = 0$,

$$\langle E_k\rangle = \frac{m}{2}\langle v_y\rangle^2 + T_y + T_x, \tag{3}$$

with $\frac{m}{2}\langle v_y\rangle^2$, $T_y = \frac{m}{2}\langle \delta v_y^2\rangle$, and $T_x = \frac{m}{2}\langle \delta v_x^2\rangle$ being the mean flow kinetic energy and the thermal kinetic energy in the mean flow and transverse directions, respectively.

We may consider thermal kinetic energy to be the granular temperature in the system. However, such definition of granular temperature makes sense only if the velocity distribution is Gaussian. By examining the probability function $P(v_y)$ of v_y at the upstream location [see inset of Fig. 5(a)], we find a bimodal distribution instead of a Gaussian distribution. On the other hand, the probability function $P(v_x)$ of v_x is closer to a Gaussian distribution. Therefore, while the particles can be considered as a granular gas in the x direction, they cannot be treated as a simple granular gas in the y direction.

Similar to Ref. [3], the bimodal distribution of $P(v_y)$ suggests a way to divide the particles into two types: (1) high speed particles with $v_y > v_c = 1$ m/s, where v_c is a threshold velocity at which the high speed peak begins, and (2) low speed particles with $v_y < v_c$. Since type-1 particles carry most of the mean flow energy, the energy transfer mentioned before can be treated as conversion of type-1 particles to type-2 particles due to interparticle collisions. The inset in Fig. 6(a) shows $P(v_y)$ measured at different locations. In the upstream position, most particles are type-1. As the particles move toward the shock, collisions between a type-1 particle and a type-2 particle will most probably result in two type-2 particles. Hence, the density of type-1 particle (n_1) decreases while that of type-2 particle (n_2) increases toward the shock. This is indeed observed in our experiment as shown in Fig. 6(a).

Using this simple model, the transverse temperature profile $T_x(y)$ may be obtained using a simple kinetic theory. In the first region at $y<y_1$ where type-1 particles outnumber type-2 particles, energy is transferred from type-1 particles to type-2 particles by collisions between them. Hence the rate of increase in T_x should be proportional to the product of n_1, n_2, and $\langle E_k\rangle$. In the comoving frame in which all the physical quantities are stationary, the rate of change is replaced by the gradient in the mean flow direction, so we have $\frac{dT_x}{dy} = \frac{c}{u}\langle E_k\rangle n_1 n_2$. Here the constant c is a measure of how efficient the energy transfer is. Then we have

$$T_x(y) = \int_0^y dy \frac{c}{u}\langle E_k\rangle n_1 n_2 + T_x(0). \tag{4}$$

Using numerical values of n_1 and n_2, the experimental value of $T_x(y)$ is found to be consistent with the above expression for $y<y_1=22$ mm with $c=0.15$ mm^{-4} s^{-1} [see Fig. 6(c)]. Presumably when $y>y_1$, $T_x(y)$ decreases due to increasing rate of dissipative collisions.

When $y>y_2=25$ mm, the type-2 particles behave as an isotropic granular gas in quasiequilibrium because the

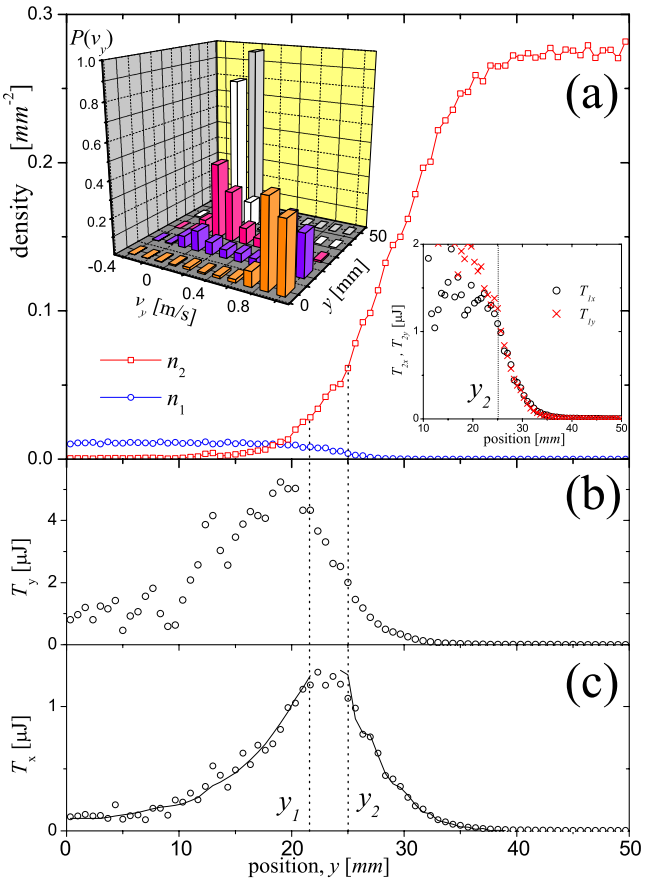

FIG. 6. (Color online) (a) Density profiles (n_1, n_2) for type-1 and type-2 particles. The upper inset shows the probability function $P(v_y)$ at different locations: $y=5$, 15, 25, 35, and 45 mm and the lower inset shows the T_2x and T_2y profiles; profiles of the thermal kinetic energy (b) T_y and (c) T_x.

granular temperatures (T_{2x}, T_{2y}) in both (x and y) directions are the same [see lower inset of Fig. 6(a)] so that $T_2=T_{2x}+T_{2y}=2T_{2x}$. Here T_2 is the type-2 particles granular gas temperature that is related to the pressure P_2 through the equation of state for granular fluids [12,13]: $P_2=n_2RT_2$ with $R=\frac{n_c+n_2}{n_c-n_2}$ where $n_c=0.267$ mm^{-2} is the random close pack density [11]. On the other hand, momentum balance in the mean flow direction gives $P_2+m(n_2v_2^2+n_1v_1^2)=C$, where $C=4.03$ μJ mm^{-2} is a constant within the granular gas. Putting the equation of state in the momentum balance equation, we have

$$T_2=\frac{n_c-n_2}{n_2(n_c+n_2)}[C-m(n_2v_2^2+n_1v_1^2)]. \tag{5}$$

Then the granular temperature in the x direction may be calculated: $T_x=fT_{1x}+(1-f)T_{2x}=fT_{1x}+(1-f)T_2/2$ with $f=\frac{n_1}{n_1+n_2}$ being the fraction of type-1 particles. The solid line in Fig. 6(c) is a predicted result, which agrees with the experimental data well. We find equally good agreement of our model to the data measured at different γ.

We also find that the granular shocks in our setup differ qualitatively from those produced in open flow situations [3]. While the width of our shock increases with inflow rate γ (see inset of Fig. 4), the shock width in Ref. [3] decreases with γ. In Boudet's setup [3] the particles flow away from the obstacle when they hit it. The particles remain in a fluid state next to the solid obstacle. High particle inflow rate implies high momentum flux and energy flux. Since the pressure is proportional to the momentum flux, increasing the influx increases the pressure and therefore reduces the thickness of the profile. On the other hand, in our setup with a closed bottom, particles behind the shock front dissipate all their energy and condense to a solid state. Unlike the solid obstacle in Ref. [3], particles in this solid state may be excited to the fluid state when being hit upon. Because it is the energy influx associated with inflowing particles that generates the granular fluid layer, the thickness of this layer should increase with the particle inflow rate. Although a higher inflow rate leads to high pressure, it is balanced by the increase in thermal pressure in this layer due to the increase in energy flux. However, further experiments are needed to check the above speculation.

To summarize, we successfully account for the temperature profile in granular shock using a simple kinetic theory in terms of energy transfer from the mean flow direction to the transverse direction. We also find that, contrary to ordinary fluids and previous granular shock experiments, the granular shock width increases with the inflow rate.

This research is supported by a special grant from the Institute of Physics (IOP) of Academia Sinica, Taipei and IOP of the Chinese Academy of Sciences (CAS), Beijing. M.H. would also like to thank support from CAS Grants No. KKCX1-YW-03 and No. KJCX2-YW-L08 and CNSF Grants No. 10720101074 and No. 10874209.

[1] H. M. Jaeger, S. R. Nagel, and R. P. Behringer, Phys. Today **49**(4), 32 (1996).
[2] E. C. Rericha, C. Bizon, M. D. Shattuck, and H. L. Swinney, Phys. Rev. Lett. **88**, 014302 (2001).
[3] J. F. Boudet, Y. Amarouchene, and H. Kellay, Phys. Rev. Lett. **101**, 254503 (2008).
[4] C. Cercignani, A. Frezzotti, and P. Grosfils, Phys. Fluids **11**, 2757 (1999).
[5] M. Hou, W. Chen, T. Zhang, K. Lu, and C. K. Chan, Phys. Rev. Lett. **91**, 204301 (2003).
[6] K. To, Mod. Phys. Lett. B **19**, 1751 (2005).
[7] *Traffic and Granular Flow in Stuttgart, Germany, 1999* edited by D. Helbing, H. J. Herrmann, M. Schreckenberg, and D. E. Wolf (Springer, Singapore, 1999).
[8] J. Rajchenbach, Adv. Phys. **49**, 229 (2000).
[9] H. T. Shen and S. Lu, *Proceedings of the Eighth International Conference on Cold Regions Engineering*, Fairbanks, Alaska, 1996 (ASCE, Fairbanks, 1996), pp. 594–605.

[10] K. Huang, G. Miao, P. Zhang, Y. Yun, and R. Wei, Phys. Rev. E **73**, 041302 (2006).
[11] N. Xu, J. Blawzdziewicz, and C. S. O'Hern, Phys. Rev. E **71**, 061306 (2005); O. Herbst, P. Muller, M. Otto, and A. Zippelius, *ibid.* **70**, 051313 (2004).
[12] J. Eggers, Phys. Rev. Lett. **83**, 5322 (1999).
[13] E. L. Grossman, Tong Zhou, and E. Ben-Naim, Phys. Rev. E **55**, 4200 (1997).